Very High Hole Mobility in P-Type Si/SiGe Modulation-Doped Heterostructures

1997 Jpn. J. Appl. Phys. 36 L323

(http://iopscience.iop.org/1347-4065/36/3B/L323)

Jpn. J. Appl. Phys. Vol. 36 (1997) pp. L 323–L 326
Part 2, No. 3B, 15 March 1997

Very High Hole Mobility in P-Type Si/SiGe Modulation-Doped Heterostructures

Wen-Chung TSAI, Chun-Yen CHANG, Guo-Wei HUANG, Frank-Fu FANG[1],
Yang-Hueng CHANG[2] and Chen-Feng HUANG[2]

Department of Electronic Engineering and Institute of Electronics,
National Chiao-Tung University, Hsin-Chu, Taiwan, R.O.C.
[1] *Center of Condensed Matter Sciences, National Taiwan University, Taipei, Taiwan, R.O.C.*
[2] *Department of Physics, National Taiwan University, Taipei, Taiwan, R.O.C.*

(Received September 9, 1996; accepted for publication February 4, 1997)

In this study, high-quality Si/Si$_{1-x}$Ge$_x$/Si p-type modulation-doped heterostructures were grown by ultrahigh-vacuum/chemical vapor deposition (UHV/CVD). High-field magnetotransport measurements revealed Shubnikov-de Hass oscillations in the longitudinal magneto resistance and the integer quantum Hall effect in transverse magnetoresistance illustrating the presence of a well-confined two-dimensional hole gas. The mobilities of the two-dimensional hole gas, as high as 12500 cm^2/V·s at 0.65 K, were obtained for normal (doped layer at surface side) modulation-doped heterostructures with $x = 0.12$ at a sheet carrier concentration of 3.45×10^{11} cm^{-2}. In addition, for this heterostructure, temperature-dependent measurements of Shubnikov-de Hass oscillations in the range 0.65 K–2.4 K were taken and the hole effective mass of $0.295m_0 \pm 0.01m_0$ was obtained.

KEYWORDS: modulation-doped heterostructure, Shubnikov-de Hass oscillation, quantum Hall effect, two-dimension hole gas, hole effective mass

The current interest in fundamental investigations of charge transport in modulation-doped Si/Si$_{1-x}$Ge$_x$ heterostructures has been focused on two-dimensional hole gases (2DHGs)$^{1-4)}$ and electron gases (2DEGs)$^{5-7)}$ in silicon-based materials, which stems from the potential for application to new devices and subsequent integration with the well-established Si technology. Besides device applications, the successful growth of high-hole-mobility structures has made possible the investigation of a number of novel physical phenomena, such as the fractional quantum Hall effect and ballistic transport. In addition, the two-dimensional hole gas mobility at low temperature in silicon grown on a silicon substrate has been dramatically improved in recent years to values of around 3300 to 19820 cm^2/V·s.$^{1,3,4)}$ The analysis of two-dimensional hole gas mobility behavior indicated that it is limited by scattering associated with charge, interface roughness and Ge composition abruptness at the Si/Si$_{1-x}$Ge$_x$/Si interface. In this letter, we report a 2DHG mobility as high as 12500 cm^2/V·s at 0.65 K with $x = 0.12$. The influence of the growth conditions on the low-temperature 2DHG mobility of coherent strained Si/Si$_{1-x}$Ge$_x$ modulation-doped heterostructures is also discussed.

The Si/SiGe heteroepitaxial layers have been grown by hot-wall UHV/CVD, owing to requirements for tight control over interfacial quality, spatial dopant distribution, and layer thickness. Details of the wafer cleaning method and the growth conditions have been described elsewhere.$^{8)}$ Herein, the Si/Si$_{1-x}$Ge$_x$/Si normal p-type modulation-doped heterostructures were grown on (100), n$^-$–type, 3-inch Si substrates at 525°C. The heterostructures consist of a 0.3-μm-thick undoped Si buffer layer, a 25 nm nominally undoped Si$_{0.88}$Ge$_{0.12}$ alloy channel layer, a 10 nm undoped Si layer spacer , and a 10 nm Si layer doped with boron to 2×10^{18} cm^{-3} grown sequentially. Both the layer thickness and Ge composition in the heterostructures were measured by high-resolution double-crystal X-ray diffraction (HRXRD); the SiGe layers were fully strained. Next, the boron concentration was determined using secondary ion mass spectroscopy (SIMS). From our SIMS measurement results, no boron contamination in undoped layers was detected throughout the modulation-doped structure. In addition the doping profile transition at the interface of the doped Si layer and undoped Si layer is very abrupt. Such a feature is due to the lower growth temperature of 525°C the lower growth rate R_{Si} was 0.3 nm/min, while R_{SiGe} was 3.0 nm/min. The pump-down time for outgassing of gas sources in our UHV/CVD chamber is about 2 seconds; hence, gas source facilities do not affect the doping profile.

To study the conduction mechanism of holes in the modulation-doped heterostructures, Shubnikov-de Hass (SdH) measurements were taken at 0.65 K–2.4 K, in magnetic fields up to 8 T. Conventional Hall methods using the standard van der Pauw pattern were used to measure magnetoresistence. Ohmic contacts were obtained by evaporation and alloying of Al on this sample at ~580°C. Figures 1(a) and 1(b) show longitudinal (ρ_{xx}) and transverse (ρ_{xy}) magnetoresistances plotted against magnetic field, $\boldsymbol{B}$, in the range of 0.65 K–2.4 K, respectively. The sample exhibited magnetoresistance oscillations at different low temperatures in SdH measurements. The transverse magnetoresistance is linear at low magnetic field, but increases with a field. In addition, the well-developed quantum Hall effect (QHE) plateaus begin to be clearly resolved with integer filling factors at 0.65 K and 0.95 K; however, they are unresolved at higher temperature. The QHE plateaus and $R_{xy}(B)$ slope imply the presence of a parallel conducting path. The necessary condition for observing SdH oscillations is $\mu_{\mathrm{H}}B \geq 1$, where μ_{H} denotes the carrier mobility and B represents the strength of the magnetic field. Figure 2 depicts the longitudinal magnetoresistance of SdH oscillations with the onset magnetic field $B \sim 0.8$ T. Therefore, the two-dimensional hole gas (2DHG) mobility is $\mu_{\mathrm{H}} \geq 12500$ cm^2/V·s at 0.65 K. Herein, the single peak corresponding to the sheet carrier concentration of $n_s \sim 3.45 \times 10^{11}$ cm^{-2} was determined from the SdH oscillation periods of ρ_{xx} vs $1/B$ in low

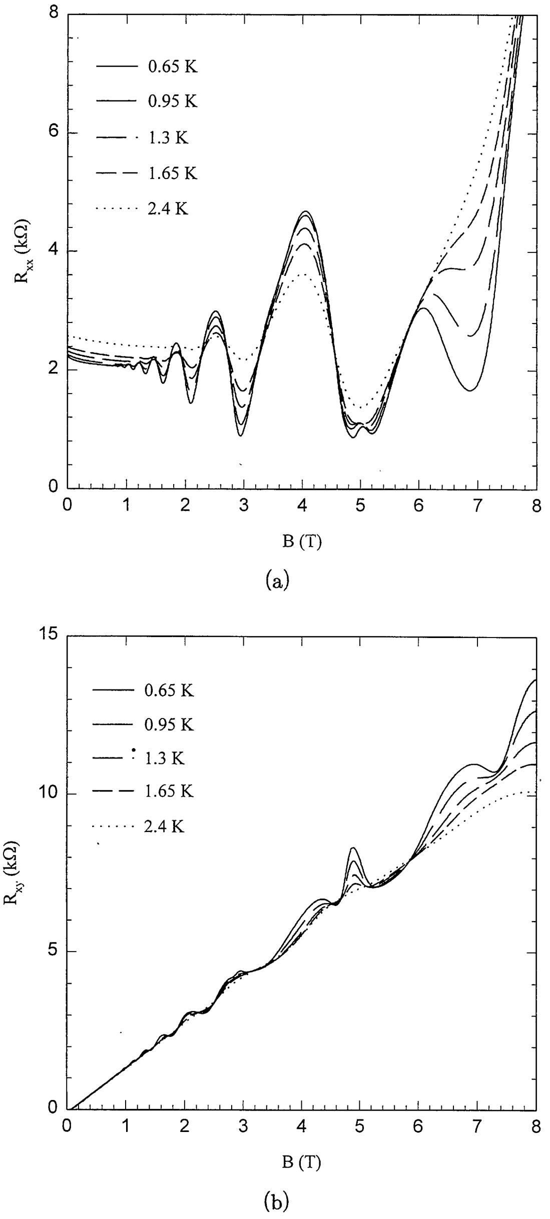

Fig. 1. (a) Longitudinal magnetoresistance vs magnetic field at different temperatures, (b) Transverse magnetoresistance vs magnetic field at different temperatures.

magnetic fields analyzed by the fast Fourier transform. The highest value of 2DHG mobility reported until now has been achieved with CVD techniques, and is comparable to that of MBE-grown samples[3,4] and theoretical calculated results[4,9] (11000–20000 $\mathrm{cm^2/V{\cdot}s}$), except for the higher sheet carrier concentration for our CVD-grown 2DHG. The hole effective mass in the heterostructures was determined from the temperature dependence of SdH oscillation amplitudes. According to these results, the amplitude of the magnetoresistance oscillation decreases with increasing temperature due to the Landau level broadening around the Fermi energy. The temperature dependence of the oscillation amplitude (A) can be expressed as

$$A \approx D_{\mathrm{T}}(\xi)\exp\left[\frac{-\pi}{\omega_{\mathrm{c}}\tau_q}\right]\times \text{const.},$$

$$D_{\mathrm{T}}(\xi)=\xi/\sinh(\xi),\ \xi=2\pi^2k_{\mathrm{B}}T/\hbar\omega_{\mathrm{c}},\ \omega_{\mathrm{c}}=\frac{eB}{m^*},\qquad(1)$$

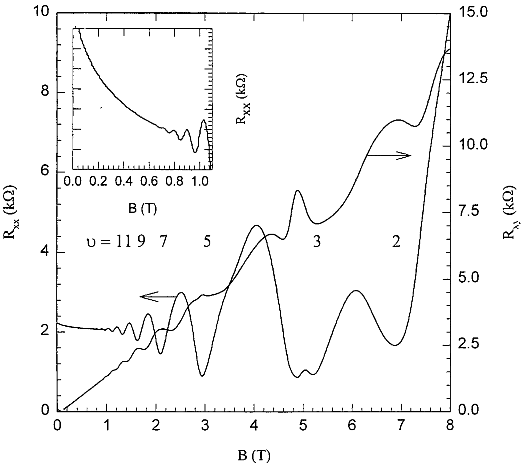

Fig. 2. Longitudinal and transverse magnetoresistance vs magnetic field at 0.65 K. The insert is a magnification to show the onset of the SdH oscillations.

where K_{B} denotes the Boltzmann constant, m^* represents the hole effective mass in 2DHG, $\hbar$ is Planck's constant and const. is temperature-independent. At low temperatures ($T < 4.2$ K), the effective mass is also independent of temperature. Therefore, the amplitude of the SdH oscillations from eq. (1) can be expressed as

$$(A/T) \cong \sinh(-2\pi^2m^*k_{\mathrm{B}}T/\hbar eB)\times \text{const.}\qquad(2)$$

The temperature dependence of SdH oscillation was measured in the range 0.65 K–2.4 K. Figure 3(a) shows plots of $\ln(\Delta R_{\mathrm{m}}/R_0)$ against $\ln(\xi/\sinh\xi)$ with 0.65 K–2.4 K for various magnetic fields $\boldsymbol{B}$, where ΔR_{m} is the peak value of ΔR_{xx}. Figure 3(b) illustrates a Dingle plot for various temperatures for this sample. Analyzing these temperature-dependent SdH oscillation amplitude data allowed us to obtained a straight line which gives the hole effective mass, $m^* \approx 0.295m_0 \pm 0.01m_0$. In addition, the effective mass is demonstrated to be independent of magnetic field and temperature. Herein, we obtain a slightly larger value for the hole effective mass than those reported by other workers.[3,10,11] This a discrepancy arises because our sample has a significantly higher carrier sheet density. However, this value corresponds to the report by People *et al.*,[1] in which the hole effective mass is $0.3m_0$, in the case of $x = 0.2$ at a sheet carrier density of $3.5\times10^{11}\ \mathrm{cm^{-2}}$, in MBE-grown $\mathrm{Si/Si_{1-x}Ge_x}$ p-type modulation-doped heterostructures.

The interface roughness, interface abruptness and alloy disorder scattering limit the magnitude of the 2DHG hole mobility. The associated modification of the V-shape potential well thickness and potential fluctuation bring about a perturbation of the eigenstate energy, giving rise to effective scattering for mobile holes. The X-ray reflectivity (XRR) and high-resolution double-crystal X-ray diffraction (HRXRD) are used to obtain parameters relevant to interface roughness, layer thickness, alloy composition and interface abruptness. Also, an X-ray reflectivity simulation program and a dynamical diffraction simulation program are implemented to analyze the experimental curves. The XRR measurements and simulation curves for a 20-period $\mathrm{Si/Si_{0.79}Ge_{0.21}}$ superlat-

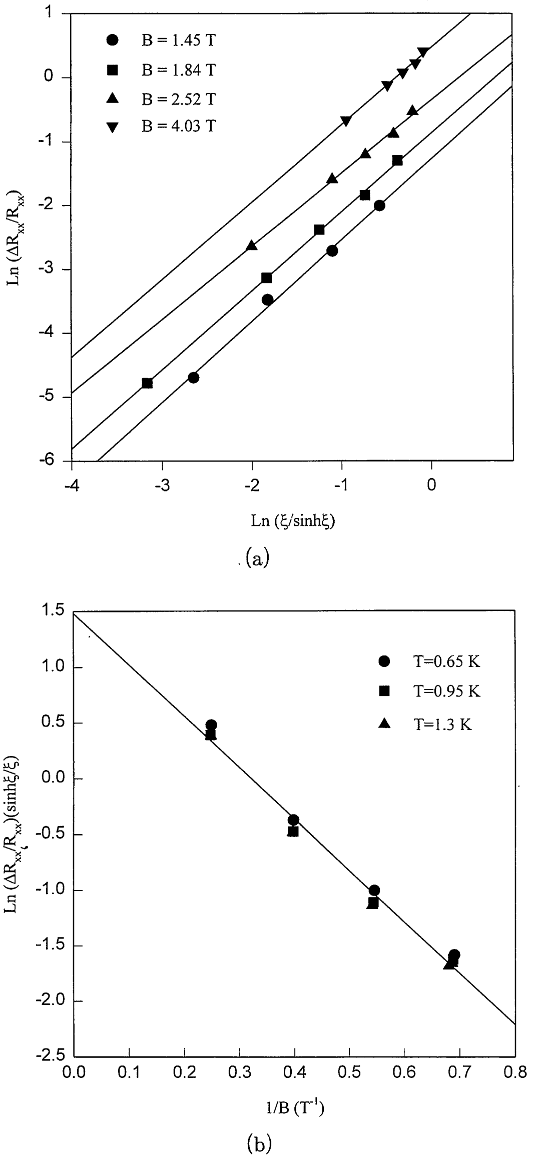

Fig. 3. (a) Plots of $\ln(\Delta R_{\rm m}/R_0)$ against $\ln(\xi/\sinh\xi)$ for various values of magnetic field $\boldsymbol{B}$. (b) Dingle plots of $\ln[(\Delta\rho_{\rm m}/\rho)(\sinh\xi/\xi)]$ as function of $1/B$ for various temperatures.

tice (SLS) with a 16.7 nm Si layer and 2.2 nm SiGe layer grown at 525°C are shown in Fig. 4. The experimental data and simulation curves correlated well with respect to the peak position, the intensity of each peak was obtained. The XRR measurements and simulations showed the $\mathrm{Si/Si_{1-x}Ge_x}$ interface roughness to be 0.1 nm for the Si layer and 0.1 nm for the SiGe layer. These values are extremely close to the XRR instrumental resolution (0.1 nm). However, the important problem is alloy composition transition at heterointerfaces, which affects the mobility of the 2DHG and the sheet density. Hence, in this study, the HRXRD measurements were taken to evaluate the structural parameters of the $\mathrm{Si/Si_{1-x}Ge_x}$ SLS.[12] A simple model has been proposed elsewhere[13, 14] to extract the Ge compositional abruptness at the $\mathrm{Si/Si_{1-x}Ge_x}$ interface. In the model, the Si/SiGe and SiGe/Si transition regions with linearly graded Ge composition is assumed at both heterointerfaces. The results obtained using this model closely correspond to the measured data. From this model, the transition region thickness can be extracted. The transition regions range from 0.34 nm to 0.66 nm (for $x = 0.14$ to 0.28) when is grown at 525°C. These values confirm that our UHV/CVD system has very fast gas transients and absence of Ge segregation,[14–16] resulting in an atomic-scale composition transition region. Hence, the coherently strained $\mathrm{Si/Si_{1-x}Ge_x}$ p-type modulation-doped heterostructures with a smooth interfacial roughness and abrupt interface have been achieved, indicating that the use of our UHV/CVD system can result in a high crystal quality and high 2DHG mobility.

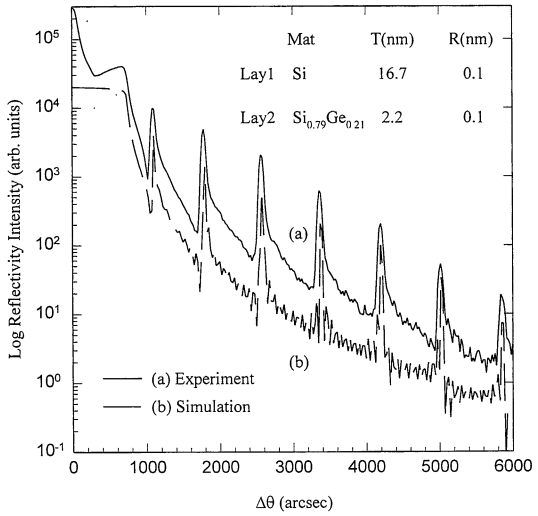

Fig. 4. The XRR reflection measurement for 20-period $\mathrm{Si/Si_{1-x}Ge_x}$ superlattice grown at 525°C. The parameters used for the simulated curves are given in the figure.

In conclusion, we have grown high-quality SiGe alloy layers at 525°C by UHV/CVD. The $\mathrm{Si/Si_{1-x}Ge_x/Si}$ p-type normal modulation-doped heterostructures are fabricated with an extremely high hole mobility and high sheet carrier concentration, and show a 2DHG hole mobility as high as 12500 $\mathrm{cm^2/V{\cdot}s}$ at 0.65 K, at a sheet carrier density $n_{\rm s}$ of $3.45 \times 10^{11}\,\mathrm{cm^{-2}}$ for $x = 0.12$. The study also reveals the hole effective mass m^* to be $0.295m_0 \pm 0.01m_0$, which is independent of temperature and magnetic field. The major factors that limit the 2DHG mobility and both the interface roughness of 0.1 nm and the alloy abruptness of 0.34 nm at the Si/SiGe heterointerface are determined. According to our results, an extremely smooth and abrupt Ge composition transition is achieved at both Si and SiGe heterointerfaces by UHV/CVD.

Acknowledgements

The authors thank Dr. M. E. Chen for XRR measurements and valuable discussions. This work was supported by the National Science Council of the Republic of China under Contract No. NSC-85-2215-E009-038.

1) R. People, J. C. Bean, D. V. Lang, A. M. Sergen, H. L. Stormer, K. W. Wecht, R. T. Lynch and K. Baldwin: Appl. Phys. Lett. **45** (1984) 1231.

2) P. J. Wang, B. S. Meyerson, F. F. Fang, J. Nocera and B. Parker: Appl. Phys. Lett. **55** (1989) 2333.
3) T. E. Whall, N. L. Mattey, A. D. Plews, P. J. Phillips, O. A. Mironov, R. J. Nicholas and M. J. Kearney: Appl. Phys. Lett. **64** (1994) 357.
4) E. Bassaran, R. A. Kubiak, T. E. Whall and E. H. C. Parker: Appl. Phys. Lett. **64** (1994) 3470.
5) F. Schäffler, D. Tobben, H-J. Herzog, G. Abstreiter and B. Hollander: Semicond. Sci. & Technol. **7** (1992) 260.
6) K. Ismail, S. F. Nelson, J. O. Chu and B. S. Meyerson: Appl. Phys. Lett. **63** (1993) 660.
7) K. Ismail, S. Rishton, J. O. Chu, S. F. Nelson and B. S. Meyerson: IEEE Electron Device Lett. **EDL-14** (1993) 348.
8) T. G. Jung, C. Y. Chang, T. C. Chang, H. C. Lin, T. Wang, W. C. Tsai, G. W. Huang and P. J. Wang: Jpn. J. Appl. Phys. **33** (1994) 240.
9) C. J. Emeleus, T. E. Whall, D. W. Smith, R. A. Kubiak and E. H. C. Parker: J. Appl. Phys. **73** (1993) 3852.
10) T. E. Whall, A. D. Plews, N. L. Mattey and E. H. C. Parker: Appl. Phys. Lett. **65** (1994) 3362.
11) S. R. Chun and K. L. Wang: IEEE Trans. Electron Devices **ED-39** (1992) 2153.
12) T. C. Chang, C. Y. Chang, T. G. Jung, W. C. Tsai, P. J. Wang, T. L. Lee and L. J. Chen: J. Appl. Phys. **75** (1994) 3441.
13) W. C. Tsai, C. Y. Chang, T. G. Jung, T. S. Liou, G. W. Huang, T. C. Chang, L. P. Chen and H. C. Lin: Appl. Phys. Lett. **67** (1995) 1092.
14) W. C. Tsai, C. Y. Chang, T. G. Jung, T. S. Liou, G. W. Huang, T. C Chang, L. P. Chen and H. C. Lin: to be published in J. Appl. Phys.
15) M. Copel and R. M. Tromp: Appl. Phys. Lett. **58** (1991) 2648.
16) M. Liehr, C. M. Greenlief, M. Offenberg and S. R. Kasi: J. Vac. Sci. & Tech. A **8** (1990) 2960.